Theoretical Study of the Adsorption of Ethylene on Alkali-Exchanged Zeolites

SOMBAT KETRAT, JUMRAS LIMTRAKUL

Laboratory for Computational & Applied Chemistry, Physical Chemistry Division, Kasetsart University, Bangkok 10900, Thailand

Received 30 August 2002; accepted 8 May 2003

DOI 10.1002/qua.10706

ABSTRACT: The structures of alkali-exchanged faujasite (X–FAU, X = Li^+ or Na^+ ion) and ZSM-5 (Li–ZSM-5) zeolites and their interactions with ethylene have been investigated by means of quantum cluster and embedded cluster approaches at the B3LYP/6-31G (*d*, *p*) level of theory. Inclusion of the Madelung potential from the zeolite framework has a significant effect on the structure and interaction energies of the adsorption complexes and leads to differentiation of different types of zeolites (ZSM-5 and FAU) that cannot be drawn from a typical quantum cluster model, $H_3SiO(X)Al(OH)_2OSiH_3$. The Li–ZSM-5 zeolite is predicted to have a higher Lewis acidity and thus higher ethylene adsorption energy than the Li–FAU zeolites (16.4 vs. 14.4 kcal/mol), in good agreement with the known acidity trend of these two zeolites. On the other hand, the cluster models give virtually the same adsorption energies for both zeolite complexes (8.9 vs. 9.1 kcal/mol). For the larger cation-exchanged Na–FAU complex, the adsorption energy (11.6 kcal/mol) is predicted to be lower than that of Li–FAU zeolites, which compares well with the experimental estimate of about 9.6 kcal/mol for ethylene adsorption on a less acidic Na–X zeolite. Int J Quantum Chem 94: 333–340, 2003

Key words: ZSM-5 zeolite; faujasite zeolite; DFT study; ethylene adsorption; embedded cluster

Introduction

Zeolites are of prime importance as catalysts for many industrial processes, due mainly to their shape selectivity and acid sites [1–9]. Cation-exchanged zeolites have been found to be potential catalysts for hydrocarbon reactions [10–19]. Of particular interest in this area of active research is the alkene adsorption on alkali-exchanged zeolite, which is the foundation of several industrially important reactions, namely, aromatization of olefins [18], formation of ethylbenzene and styrene [19], and the production of xylene [20].

The importance of metal-exchanged zeolites suggests that a better understanding of the structure and mechanistic properties at the molecular level of the catalyst is certainly required [21]. A review of

Correspondence to: J. Limtrakul; e-mail: fscijrl@ku.ac.th

quantum chemical calculations applied to zeolites and their interaction with unsaturated hydrocarbon has been recently reported [22]. All early works of adsorption of C_2H_4 on bare zeolite clusters were limited to small model fragments that are not specific to a particular zeolite but represent a generic tetrahedral subunit in an unconstrained environment [22–26]. It is known that small zeolitic clusters may inadequately reflect adsorption complexes at the active site and the cluster environment may enhance binding energy and, hence, more accurately predict the structures of reaction intermediates, transition states, and products [5, 27].

To include the effects of the zeolite framework on adsorption of C_2H_4 in zeolites, a periodic electrostatic structure method can be utilized [28–31]. This corresponds to the high loading case and is often computationally expensive for most zeolites due to their relatively large unit cells.

Alternatively, the embedded cluster approach [5, 9] provides a more practical methodology with little additional computational cost when compared to the bare cluster calculation. To the best of our knowledge, no theoretical work regarding the metal-exchanged zeolite–ethylene complex has been carried out so far.

In this study, we examine the effects of cations and the zeolitic framework on the adsorption properties of ethylene in alkali-exchanged faujasite and ZSM-5 using the embedded cluster methodology.

Methods

Zeolites have elementary building units of tetrahedral SiO_4 and AlO_4 commonly called T atoms. A 3-D framework of faujasite-type zeolite is built on 24-T cubo-octahedral sodalite cages linked via their six-membered rings forming large cavities called supercages [Fig. 1(a)]. On the other hand, the ZSM-5 zeolite framework is built on connected pentasil units forming straight and sinusoidal pore systems [Fig. 1(b)].

We employed the clusters illustrated in Figures 2–4 as the models of interaction of unsaturated hydrocarbon on alkali–metal-exchanged zeolites. The models $H_3SiO(X)Al(OH)_2OSiH_3$, where X = Li and Na, will hereafter be referred to as [Li–FAU], [Na–FAU], and [Li–ZSM-5], and their complexes, $H_3SiO(X)Al(OH)_2OSiH_3/[C_2H_4]$, will be referred to as [Li–FAU]/$[C_2H_4]$, [Na–FAU]/$[C_2H_4]$, and [Li–ZSM-5]/$[C_2H_4]$. The bare quantum clusters are specifically modeled according to crystallographic structures of active sites in faujasite [31] and ZSM-5 [32] zeolites. In these models, the dangling bonds of the Si atoms are terminated by H atoms and the Si—H bonds are aligned with the corresponding S—O bonds of the structures of zeolites, respectively. The naked alkali–cation/C_2H_4 adducts, Li^+/$[C_2H_4]$ and Na^+/$[C_2H_4]$, are also included for comparison with the effect of the negative zeolite oxygen framework surrounding the alkali cations.

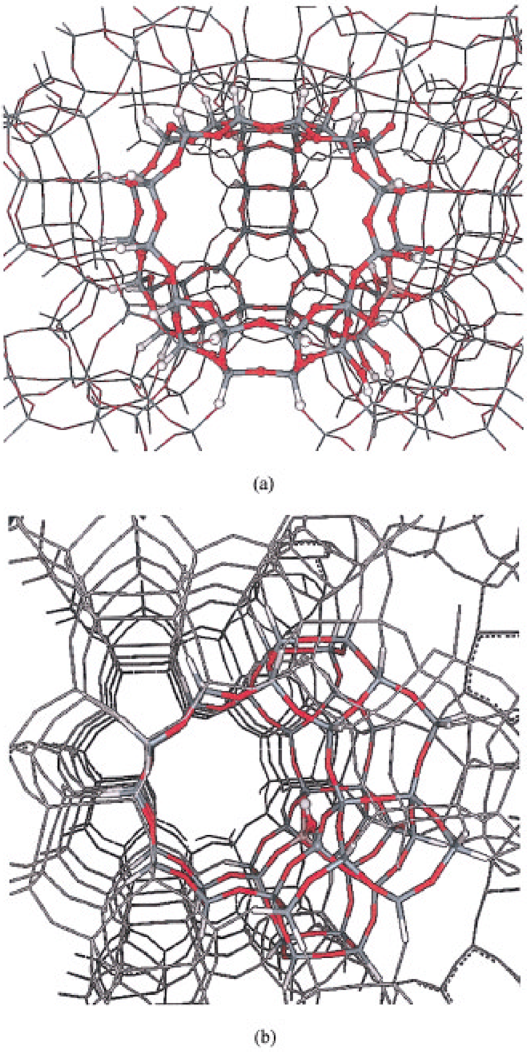

FIGURE 1. Presentation of zeolite structure. (a) Structure of faujasite showing the supercage. (b) Structure of ZSM-5 viewed from the straight direction. [Color figure can be viewed in the online issue, which is available at www.interscience.wiley.com.]

In the embedded cluster model (cf. Fig. 5), the static Madelung potential due to atoms outside of the quantum cluster is represented by charges located at the zeolite lattice sites. Charges close to the

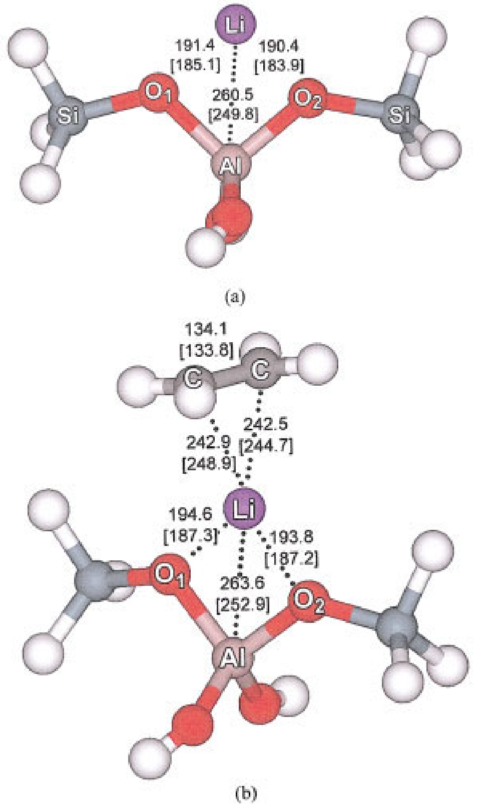

FIGURE 2. Li–FAU zeolite structures and their interaction with ethylene optimized at B3LYP/6-31G(*d*, *p*) using embedding and cluster calculations (values in parentheses); bond distances in pm. (a) Li–FAU. (b) Li–FAU/C_2H_4. [Color figure can be viewed in the online issue, which is available at www.interscience.wiley.com.]

quantum cluster are treated explicitly, while the Madelung potential from the remaining charges from an infinite lattice is represented by a set of surface charges that were derived from the surface charge representation of external embedded potential (SCREEP) method. More details on our method can be found elsewhere [5, 9]. For faujasite, the total Madelung potential is represented by 288 explicit charges and 960 surface charges, whereas for ZSM-5 the potential is represented by 360 explicit charges and 240 surface charges. With this small number of point charges, the additional computational cost is often less than 5% when compared to bare cluster calculations.

Geometry optimizations were carried out at the B3LYP level using the 6-31G (*d*, *p*) basis with the Gaussian 98 program [33]. The computations were carried out on PC clusters at the KU Computing Center and a DEC alpha station 250 workstation at the Laboratory for Computational and Applied Chemistry at Kasetsart University and a cluster of IBM RISC/6000 workstations at the Henry Eyring Center for Theoretical Chemistry, University of Utah.

Results and Discussion

METAL-EXCHANGED FAUJASITE (X-FAU)

Li–Zeolite (Li–FAU)

Cluster and embedded cluster models for alkali–metal-exchanged zeolites are shown in Figures

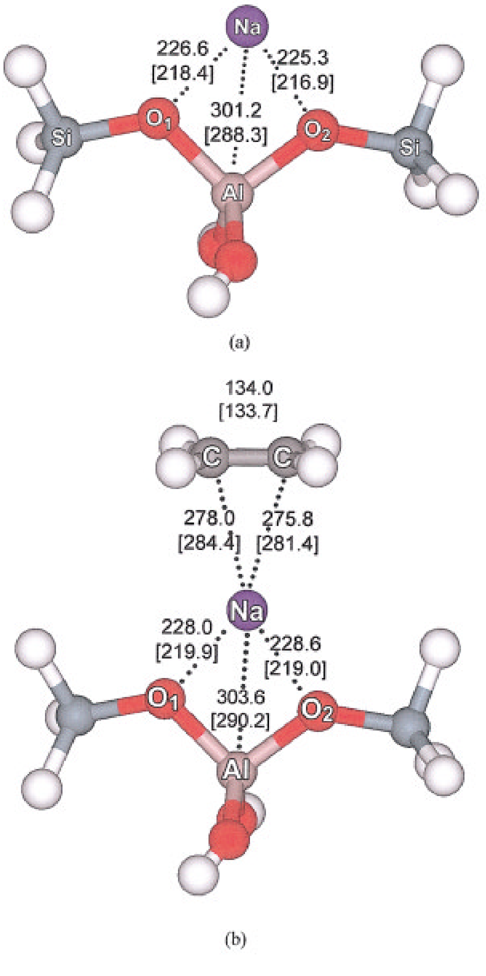

FIGURE 3. Na–FAU zeolite structures and their interaction with ethylene optimized at B3LYP/6-31G(*d*, *p*) using embedding and cluster calculations (values in parentheses); bond distances in pm. (a) Na–FAU. (b) Na–FAU/C_2H_4. [Color figure can be viewed in the online issue, which is available at www.interscience.wiley.com.]

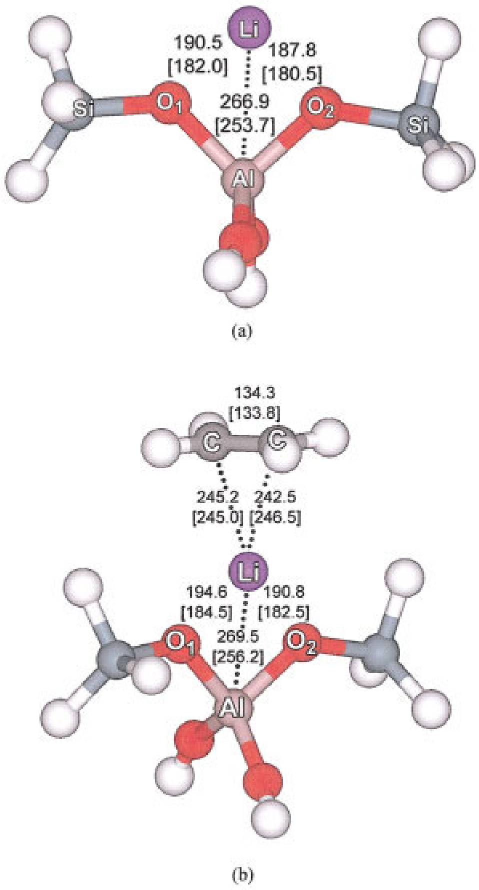

FIGURE 4. Li–ZSM-5 zeolite structures and their interaction with ethylene optimized at the B3LYP/6-31G(*d*, *p*) level using embedding and cluster calculations (values in parentheses); bond distances in pm. (a) Li–ZSM-5. (b) Li–ZSM-5/C_2H_4. [Color figure can be viewed in the online issue, which is available at www.interscience.wiley.com.]

2(a)–4(a). Selected optimized geometric parameters and atomic charges for bare quantum cluster and embedded cluster models are documented in Tables I and II. For the Li–FAU zeolite [see Fig. 2(a)], the alkali–metal cation does not bind with a particular bridging oxygen atom in the $[AlO_4]^-$ but is symmetrically bidentated to O1 and O2 of $[AlO_4]^-$ tetrahedron, in agreement with the previously reported ESR experiment [34]. The interaction of the cationic metal with the zeolite framework leads to substantial perturbation of the active acidic site. In particular, we found that the Al—O distances were elongated by 2.3 pm, but by only 0.9 pm for the Al—O2 and Al—O1 distances, respectively, while the Si—O bonds were shortened by 3.6 and 4.0 pm for the Si—O1 and Si—O2 bonds, respectively, but there was no significant change for the O1—Al—O2 angle. A reciprocal effect is that the zeolite framework reduces the Li charge. The charge on Li^+ cation was reduced to 0.53, and 0.63 a.u. for the bare cluster and the embedded models, respectively. The increase of charges on Li cation is clearly observed by the changes of charges on Al and Si atoms of the Li–FAU complexes as compared to the corresponding charges of their anionic framework (cf. Table II). The Madelung potential was found to have a significant effect on the structure of Li-exchanged FAU. In particular, it elongates the Li—Al by 10.7 pm. The extent of Li· · ·O distances increased with the embedded model (Li· · ·O1 = 185.1 pm vs. 191.4 pm and Li· · ·O2 = 183.9 pm vs. 190.4 pm). This indicates that the Madelung field weakens the attachment of the Li cation to the zeolite framework, and thus reduces the strength of the complexes, which is reflected by lower complexation energy (−135.92 kcal/mol) of Li(I) and zeolitic anion than those obtained from the bare quantum cluster (−160.78 kcal/mol).

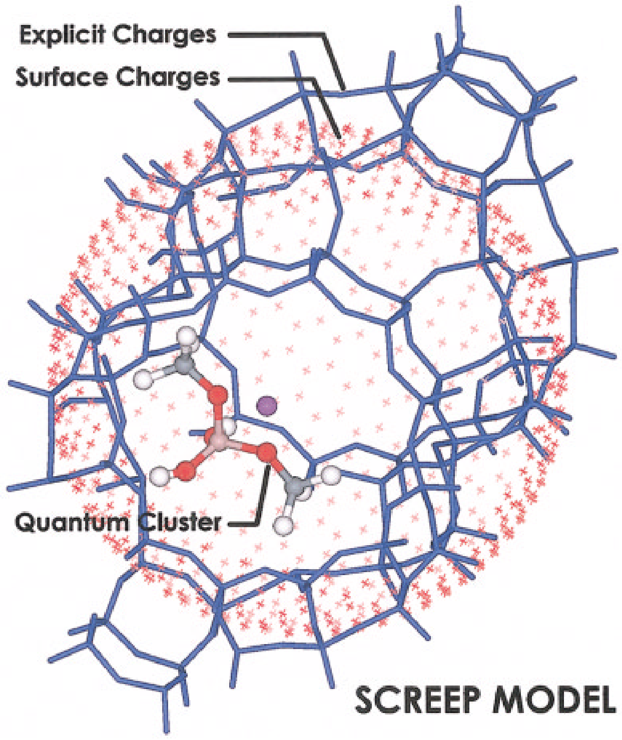

FIGURE 5. SCREEP embedded cluster model. [Color figure can be viewed in the online issue, which is available at www.interscience.wiley.com.]

TABLE I

B3LYP/6-31G(*d, p*)-optimized geometric parameters of the Li–ZSM-5, Li–FAU, and Na–FAU zeolites systems.

	[Li–ZSM-5]		[Li–FAU]		[Na–FAU]	
Parameters	Bare	Embedded	Bare	Embedded	Bare	Embedded
X^+—Al	253.7	266.9	249.8	260.5	288.3	301.2
X^+—O1	182.0	190.5	185.1	191.4	218.4	226.6
X^+—O2	180.5	187.8	183.9	190.4	216.9	225.3
O1-X^+-O2	88.4	83.5	92.2	88.6	76.8	73.6
Al—O1	176.8	178.5	180.2	181.1	179.3	180.4
Al—O2	177.1	178.3	180.8	183.1	180.0	182.3
O1-Al-O2	91.1	89.9	94.9	94.2	97.6	96.5
Si—O2	164.3	160.7	166.7	162.7	165.1	161.3
Si—O1	164.1	160.0	166.6	163.0	164.8	161.5
qX^+	0.52	0.63	0.53	0.63	0.67	0.73

Bond lengths are in pm and bond angles in degrees.

Na–Zeolite (Na–FAU)

A similar trend has been observed for the Na–FAU complex [see Fig. 3(a)] (cf. Tables I and II). The charges on the Na^+ cation within the zeolite models are 0.67 and 0.73 for cluster and embedded cluster models, respectively. The Na· · ·O distances are elongated with the embedded model (Na· · ·O1 = 218.4 pm vs. 226.6 pm and Na· · ·O2 = 216.9 pm vs. 225.3 pm). The calculated Na· · ·Al distance of the embedded model is 12.9 pm larger than that of the bare cluster, indicating that the embedding environment weakens the attachment of the metal cation to the zeolite framework. Regarding the energetics of the Na–FAU complexes, the complexation energy of the Na cation to the zeolitic framework leads to change in the geometric structures (the O1—Al—O2 bond angles and X+—Al distances, the distance between the cation and the A1 atom of zeolite framework, are increased with the increasing cationic size). These are, as expected, smaller than those for the Li–FAU complex (cf. Table II). The complexation energies of the monovalent ions Li^+ and Na^+ that are bound to a zeolitic framework are −135.92 (Li–FAU) and −118.19 (Na–FAU) kcal/mol at the embedded cluster models, following the conventional electrostatic trend. We found that the extended structure decreases the complexation energy by 24.86 kcal/mol in the Li–FAU and by 17.43 kcal/mol in the Na–FAU zeolites. This implies that the complexation energy of alkali cation bound to FAU zeolites cannot be obtained accurately by small bare quantum cluster models.

TABLE II

Atomic charges of Li–FAU and Na–FAU complexes.

	Bare cluster			Embedded cluster		
Atoms	Isolated	Li–FAU	Na–FAU	Isolated	Li–FAU	Na–FAU
Si1	0.67	0.74	0.74	1.34	1.23	1.23
Si2	0.69	0.73	0.73	1.27	1.25	1.23
O1	−0.66	−0.79	−0.76	−0.61	−0.75	−0.72
O2	−0.67	−0.79	−0.77	−0.61	−0.75	−0.73
Al	0.80	0.99	0.89	0.76	0.90	0.83
Cation	1.00	0.53	0.67	1.00	0.63	0.73
Complexation energy (kcal/mol)	—	−160.78	−135.62	—	−135.42	−118.19

TABLE III

B3LYP/6-31G(*d, p*)-optimized geometric parameters of the complex of ethylene with naked Li^+, Li–ZSM-5, Li–FAU, naked Na^+ and Na–FAU zeolites.

	Li^+/C_2H_4	Li–ZSM-5/C_2H_4		Li–FAU/C_2H_4		Na^+/C_2H_4	Na–FAU/C_2H_4	
Parameters	Naked	Bare	Embedded	Bare	Embedded	Naked	Bare	Embedded
C═C[a]	134.5	133.8	134.3	133.8	134.1	134.3	133.7	134.0
X^+—C1	238.3	245.0	245.2	248.9	242.9	272.2	284.4	278.0
X^+—C2	238.5	246.5	242.5	244.7	242.5	272.2	281.4	275.8
X^+—(C═C)[b]	228.7	236.5	233.1	237.6	233.3	263.8	274.9	268.6
Al—X^+	—	256.2	269.5	252.9	263.6	—	290.2	303.6
X^+—O1	—	184.5	194.6	187.3	194.6	—	219.9	228.0
X^+—O2	—	182.5	190.8	187.2	193.8	—	219.0	228.6
O1-X^+-O2	—	87.0	82.2	90.5	86.9	—	76.0	72.7
Al—O1	—	176.3	177.8	179.7	180.5	—	179.0	180.0
Al—O2	—	176.7	177.7	180.2	182.5	—	179.6	181.9
O1-Al-O2	—	91.4	90.4	95.3	94.8	—	97.8	96.7
Si—O1	—	163.5	159.3	166.1	162.5	—	164.5	161.2
Si—O2	—	163.9	160.3	166.1	161.8	—	164.8	160.8
qX^+	0.69	0.30	0.36	0.32	0.36	0.77	0.52	0.54

Bond lengths are in pm and bond angles in degrees.

[a] The calculated B3LYP/6-31G(*d*, *p*) of C═C bond distance in the gas phase is 133.0 pm.

[b] The distances between Li cation to the midpoint of the C═C bond.

INTERACTION OF METAL-EXCHANGED FAUJASITE (X–FAU) WITH ETHYLENE

Interaction of Li–Zeolite (Li–FAU) with Ethylene

Cluster and embedded cluster models for the adsorption of ethylene on alkali metal-exchanged zeolites are illustrated in Figures 2(b)–4(b). Selected geometric parameters of the adduct complexes are listed in Table III. Adsorption energies have been evaluated by employing different models and are given in Table IV.

For the Li–FAU/C_2H_4 zeolite [see Fig. 2(b)], the optimized Li$\cdots C_2H_4$ distances between Li cation to the midpoint of the C═C bond are found to be 233.3 and 237.6 pm, and the corresponding energies are 14.35 and 9.08 kcal/mol with basis set superposition error (BSSE) correction for the embedded cluster and quantum cluster, respectively. It is interesting to compare the adsorption of C_2H_4 on Li–FAU zeolite with the case where the zeolite framework is absent, i.e., in the naked Li–C_2H_4 system. As expected, C_2H_4 binds more strongly by a factor of 2 to the Li^+ cation (23.15 kcal/mol) than in the Li–FAU zeolite in the binding energy. The simple naked Li–C_2H_4 model obviously overestimates the interaction of C_2H_4 in a real Li-exchanged–FAU system due to the large electrostatic field generated by the naked Li cation. The bare cluster model causes a large reduction of the positive charge of the Li cation and, thus, possibly underestimates the interaction of C_2H_4 with the Li-exchanged–FAU system. The embedding environment improves the results of the bare cluster

TABLE IV

Calculated adsorption energies (kcal/mol) of C_2H_4 on naked Li^+, Na^+, bare quantum cluster, and embedded cluster model of Li–ZSM-5, Li–FAU, and Na–FAU zeolites.

	Li^+/C_2H_4	Li–ZSM-5/C_2H_4		Li–FAU/C_2H_4		Na^+/C_2H_4	Na–FAU/C_2H_4	
	Naked	Bare	Embedded	Bare	Embedded	Naked	Bare	Embedded
ΔE	−24.83	−11.55	−18.98	−11.58	−16.87	−17.76	−9.42	−13.76
ΔE_{BSSE}	−23.15	−8.94	−16.41	−9.08	−14.35	−15.97	−7.35	−11.63

model. One can see that the adsorption energy of the embedded cluster model lies between those of the bare quantum cluster model and the simple naked Li/C_2H_4 system.

Interaction of Na–Zeolite (Na–FAU) with Ethylene

For the cluster model [see Fig. 3(b)], the adsorption energy of Na–FAU/C_2H_4 complexes is calculated to be 7.35 kcal/mol lower than that of the Li–FAU/C_2H_4 complex (9.08 kcal/mol); this may be attributed to its large cationic size (relative to Li^+), which causes its interactions to be weaker than that of the Li complex. We found that the Madelung potential increases the adsorption energy by 5.27 kcal/mol in the Li–FAU and by 4.28 kcal/mol in the Na–FAU zeolites. With the inclusion of BSSE correction and the effects of the Madelung potential, we predict that the Li–FAU/C_2H_4 complex is more stable by about 2.72 kcal/mol compared to the Na–FAU/C_2H_4 complex. The adsorption energy is predicted to be 11.63 kcal/mol for the embedded cluster model of the Na–FAU/C_2H_4, which compares well with the experimental value of 9.6 kcal/mol for the less acidic Na–X zeolite complex [35]. The lower adsorption energy in Na–X zeolite, which is an aluminum-rich faujasite zeolite with an Si/Al ratio in a range of 1–1.5, corresponds to the lower acid strength of the Na–X zeolite because the acid strength of zeolite decreases as the aluminum content increases.

Effect of the Zeolite Framework on the Adsorption Properties of Ethylene

Another point of interest is the comparison of the results obtained using both cluster and embedded cluster models for exploring the different types of zeolites (faujasite and ZSM-5). Faujasite is considered a large-pore-size zeolite with a pore diameter of 74 pm and spacious supercages with a diameter of 130 pm, while ZSM-5 is a middle-pore-size zeolite with a pore diameter of about 50 pm. Although the two types of zeolites have different crystal structures (see Fig. 1), the cluster models give virtually the same adsorption energies (9.08 vs. 8.94 kcal/mol) for both Li–FAU/C_2H_4 [cf. Fig. 2(b)] and Li–ZSM-5/C_2H_4 [cf. Fig. 4(b)] complexes as listed in Table IV.

We found that inclusion of the Madelung potential increases the adsorption energy by 7.47 and 5.27 kcal/mol for the Li–ZSM-5 and Li–FAU zeolites, respectively. With the inclusion of BSSE correction and the effects of the Madelung potential, the Li–ZSM-5/C_2H_4 complex is more stable by about 2.06 kcal/mol as compared to the Li–FAU/C_2H_4 complex. Thus, the Madelung potential was found to reveal that adsorption properties of zeolite do not depend only on the acidic site center but also on the framework structure where the acidic site is located.

Conclusion

The structures of alkali-exchanged faujasite (X–FAU, X = Li^+, or Na^+ ion) and ZSM-5 (Li–ZSM-5) zeolites and their interaction with ethylene have been investigated by means of both the quantum cluster and embedded cluster approaches at the B3LYP/6-31G (*d*, *p*) level of theory. The effects of the Madelung potential were found to be important. The bare quantum cluster is too small to account for the extended structure and, therefore, yields almost the same binding energies (8.94 vs. 9.08 kcal/mol) for both Li–ZSM-5/C_2H_4 and Li–FAU/C_2H_4 complexes. On the other hand, the binding energy derived from the embedded model of Li–ZSM-5/C_2H_4 is calculated to be 16.41 kcal/mol, which is larger than that obtained from the Li–FAU complex (14.35 kcal/mol), indicating that the metal-exchanged ZSM-5 is more acidic than the metal-exchanged FAU zeolites and leads to a better agreement with the experimental observation. The ion (X)· · ·Al distance increases with the increase in ionic radii. The predicted adsorption energy for Na–FAU/C_2H_4 (11.63 kcal/mol) is comparable with the experimental estimate of about 9.6 kcal/mol for ethylene adsorbed on Na–X zeolite. The results obtained in the present study suggest that the embedded cluster approach yields a more accurate and practical model than the bare quantum cluster for exploring the zeolite framework and catalytic properties.

ACKNOWLEDGMENTS

This work was supported by the Thailand Research Fund (TRF) in supporting the TRF Senior Research Scholar to J.L., by ADB-MUA, and by the Kasetsart University Research and Development Institute (KURDI). Sincere thanks are extended to Professor R. Ahlrichs (Karlsruhe, Germany) and Professor T. N. Truong (University of Utah, Salt

Lake City, UT) for their continued support of this work.

References

1. Catlow, C. R. A. Modeling of Structure and Reactivity in Zeolites; Academic: San Diego, 1992.
2. van Santen, R. A.; Kramer, G. J. Chem Rev 1995, 95, 637.
3. Limtrakul, J. Chem Phys 1995, 193, 79.
4. Limtrakul, J.; Treesukol, P.; Probst, M. Chem Phys 1997, 215, 77.
5. Limtrakul, J.; Nanok, T.; Jungsuttiwong, S.; Khongpracha, P.; Truong, T. N. Chem Phys Lett 2001, 349, 161.
6. Limtrakul, J.; Tantanak, D. Chem Phys 1996, 208, 331.
7. Zygmunt, J. A.; Curtiss, L. A.; Iton, L. E.; Erhardt, M. K. J Phys Chem 1996, 100, 6663.
8. Krossner, M.; Sauer, J. J Phys Chem 1996, 100, 6199.
9. Treesukol, P.; Troung, T. N.; Limtrakul, J. J Phys Chem B 2001, 105, 2421.
10. Barthomeuf, D. Catal Rev 1996, 38, 521.
11. Maxwell, I. E. Adv Catal 1982, 31, 1.
12. Engelhardt, J.; Szani, J.; Valyon, J. J Catal 1987, 107, 29.
13. Hathaway, P. E.; Davis, M. E. J Catal 1989, 119, 497.
14. Corma, A. Mater Res Soc Symp Proc 1991, 233, 17.
15. Hölderich, W. F.; Hesse, M.; Naümann, F. Angew Chem 1988, 27, 226.
16. Fu, Z. H.; Ono, Y. Catal Lett 1993, 21, 43.
17. Sidorenko, Y. N.; Galich, P. N.; Gutyrya, V. S.; Il'in, V. G.; Neimark, I. E. Dokl Akad Nauk SSSR 1967, 173, 132.
18. Huang, M.; Kaliaguine, S. J Mol Catal 1993, 81, 37.
19. Yashima, T.; Sato, K.; Hayasaka, H. T.; Hara, N. J Catal 1972, 26, 303.
20. Kanzansky, V. B. Catal Today 1999, 51, 419.
21. Deka, R. C.; Hirao, K. J Mol Catal A 2002, 181, 275.
22. Boronat, M.; Viruela, P.; Corma, A. J Phys Chem A 1998, 102, 982.
23. Kazansky, V. B. Acc Chem Res 1991, 24, 379.
24. Evleth, E. M.; Kassab, E.; Jessri, H.; Allavena, M.; Montero, L.; Sierra, L. R. J Phys Chem 1996, 100, 11368.
25. Ugliengo, P.; Ferrari, A. M.; Zecchina, A.; Garrone, E. J Phys Chem 1996, 100, 3632.
26. O'Malley, P. J.; Franworth, K. J. J Phys Chem 1998, 102, 4507.
27. Greatbanks, S. P.; Hillier, I. H.; Burton, N. A.; Sherwood, P. J Chem Phys 1996, 105, 3370.
28. Dovesi, R.; Saunders, V. R.; Roetti, C. Crystal 92, an ab initio Hartree–Fock LCAO Program for Periodic Systems; Theoretical Chemistry Group, University of Torino and SERC, Daresbury Laboratory: Torino, Italy, 1992.
29. Campana, L.; Selloni, A.; Weber, J.; Pasquarello, A.; Papai, I.; Goursot, A. Chem Phys Lett 1994, 226, 245.
30. Teunissen, E. H.; Roetti, C.; Pisani, C.; de Man, A. J. M.; Jansen, A. P. J.; Orlando, R.; van Santen, R. A.; Dovesi, R. Model Simul Mater Sci Eng 1994, 2, 921.
31. Mortier, W. J.; van der Bosche, E.; Uytherhoven, J. B. Zeolites 1984, 4, 41.
32. van Koningveld, H.; van Bekkum, H.; Jansen, J. C. Acta Crystallogr B 1987, 43, 127.
33. Frisch, M. J.; Trucks, G. W.; Schlegel, H. B.; Scuseria, G. E.; Robb, M. A.; Cheeseman, J. R.; Zakrzewski, V. G.; Montgomery, J. A.; Stratmann, R. E. Jr.; Burant, J. C.; Dapprich, S.; Millam, J. M.; Daniels, A. D.; Kudin, K. N.; Strain, M. C.; Farkas, O.; Tomasi, J.; Barone, V.; Cossi, M.; Cammi, R.; Mennucci, B.; Pomelli, C.; Adamo, C.; Clifford, S.; Ochterski, J.; Petersson, G. A.; Ayala, P. Y.; Cui, Q.; Morokuma, K.; Salvador, P.; Dannenberg, J. J.; Malick, D. K.; Rabuck, A. D.; Raghavachari, K.; Foresman, J. B.; Cioslowski, J.; Ortiz, J. V.; Baboul, A. G.; Stefanov, B. B.; Liu, G.; Liashenko, A.; Piskorz, P.; Komaromi, I.; Gomperts, R.; Martin, R. L.; Fox, D. J.; Keith, T.; Al-Laham, M. A.; Peng, C. Y.; Nanayakkara, A.; Challacombe, M.; Gill, P. M. W.; Johnson, B.; Chen, W.; Wong, M. W.; Andres, J. L.; Gonzalez, C.; Head-Gordon, M.; Replogle, E. S.; Pople, J. A. Gaussian 98; Gaussian, Inc.; Pittsburgh, PA, 2001.
34. Hosono, H.; Kawazoe, H.; Nishii, J.; Kanazawa, J. J Non Cryst Solid 1982, 51, 217.
35. Carter, J. L.; Yates, D. J. C.; Lucchesi, P. J.; Elliott, J. J.; Kevorkian, V. J Phys Chem 1996, 70, 1126.